https://doi.org/10.3311/PPci.20586

Periodica Polytechnica Civil Engineering, 67(1), pp. 65–79, 2023

Experimental and FEM Analysis for Fracture Performance Evaluation of Concrete Made with Recycled Construction and Demolition Waste Aggregates

P. N. Ojha[1], Pranay Singh[1*], Brijesh Singh[1], Abhishek Singh[1], Ajay[1], Amit Sagar[1]

[1] Centre for Construction Development & Research, National Council for Cement and Building Materials, Faridabad, 121004, India
[*] Corresponding author, e-mail: cdrb@ncbindia.com

Received: 02 June 2022, Accepted: 27 September 2022, Published online: 03 October 2022

Abstract

Paper presents experimental and Finite Element Method (FEM) analysis of fracture behavior of concrete made using Recycled Aggregate (RA). Concrete mixes were prepared using Construction and Demolition Waste (CDW) as replacement of natural coarse aggregates. To study fracture performance, concrete mixes were prepared with water to cementitious content (w/b) ratios between 0.4 and 0.5. Beam specimens of size 100 mm x 100 mm x 500 mm were cast and tested as per method of Three-point bend test on notched beam proposed by RILEM. Fracture parameters like fracture energy, stress intensity factor, energy release rate and characteristic length were evaluated using Load-CMOD (Crack Mouth Opening Displacement) and load deformation curves. Mechanical properties of concrete such as compressive and flexural strength, modulus of elasticity and split tensile strength were also evaluated. The performance of concrete using RA has been compared with concrete using Natural Aggregate (NA) from literature. Results suggest slightly better fracture performance in case of concrete made using RA in comparison to conventional concrete in spite of having similar strength and w/b ratio. Fracture energy parameter in terms of stress intensity factor obtained from FEM analysis were similar to experimental results wherein no significant variation in stress intensity factor for concrete mixes with recycled and natural aggregate were observed. However, it can be stated that values of stress intensity factor of 0.47_NA was lowest and 0.5_RA was highest. There was no significant difference in average fracture energy of mixes and it lies in range of 180 N/m to 300 N/m.

Keywords

recycled aggregate concrete, fracture energy, CMOD, notched-beam, characteristic length

1 Introduction

In recent years, application of Recycled Aggregate (RA), from Construction and Demolition Waste (CDW) in structural concrete has been widely discussed topic among the researchers [1]. Ojha et al. [1] presented a perspective on construction and demolition waste aggregate concrete production and its utilization in concrete. Authors suggested a need for proper standardization for full scale construction applications. Silva et al. [2] reviewed 236 literatures published from 1997 to 2014 and summarized various factors affecting properties of recycled aggregates for concrete production. Based on the findings, the study concludes certain factors which must be considered while collection and use of RA. Wagih et al. [3] studied the feasibility of transforming and using concrete rubble into recycled aggregate for use in structural concrete. Study found water absorption and abrasion resistance of RA to be lower than the prescribed Egyptian standard code. Also, full replacement of Natural Aggregate (NA) by RA reduced the workability as well as the strength of the concrete significantly. Whereas replacement of NA by 25% to 50% of RA showed only minor reduction in the strength of the concrete. Rao et al. [4] in their study presented a global preview on the management of construction and demolition waste, properties of the recycled aggregate and concrete prepared from it and concluded with various obstacle in its widespread use. The study suggested that RA can be used for making normal structural concrete with addition of fly ash, condensed silica fume etc. Literature about the characterization and properties of recycled aggregates and recycled aggregate concrete are widely available. Martín-Morales et al. [5] performed the characterization of recycled aggregate from construction and demolition waste for

Cite this article as: Ojha, P. N., Singh, P., Singh, B., Singh, A., Ajay, Sagar, A. " Experimental and FEM Analysis for Fracture Performance Evaluation of Concrete Made with Recycled Construction and Demolition Waste Aggregates", Periodica Polytechnica Civil Engineering, 67(1), pp. 65–79, 2023. https://doi.org/10.3311/PPci.20586

production of concrete as per the Spanish code EHE-08. Recycled aggregates were evaluated based on geometric, physical, mechanical, and chemical properties. Geometric and physio mechanical properties satisfied the limit of codal provisions, but the chemical composition was not satisfactory due to high amount of sulfate and chlorides. Authors suggested to use recycled aggregates in combination with natural aggregates to overcome its minor limitations. Alexandridou et al. [6] studied the mechanical and durability performance of concrete made with recycled aggregates in proportions ranging from 0% to 75%. Study found a higher percentage of SiO_2, Al_2O_3, Fe_2O_3 and alkali oxide in RA. However, water-soluble ions which may affect the setting time of cement, were not found. The study concluded that use of coarse RA reduces the durability of concrete and water absorption tends to increase linearly with increase in percentage of coarse aggregate replacement. Bravo et al. [7] performed an analysis on the microstructure of concrete with recycled aggregates from construction and demolition waste from different sources in Portugal. Study concluded that the bonding capacity of the aggregate to cement paste is greatly influenced by the nature of RA. Increase in the water absorption was also reported with replacement of NA with RA in the concrete. Ahmed [8] studied the properties of concrete with varying percentages of RA in concrete containing fly ash. Study concluded that workability of RA based concrete decreased with increase in RA content. Addition of fly ash in the Recycled Concrete Aggregate (RCA) based concrete mix resulted in improved workability and long-term compressive strength along with a reduced water absorption value. Angulo et al. [9] classified the mixed C&D waste on the basis of its porosity and studied its impact on the mechanical performance of the concrete. Study suggested that the Young's modulus of elasticity and compressive strength follow an exponential relationship with the porosity of coarse C&D aggregates, considering other mix parameters remains constant.

Ossa et al. [10] conducted a number of tests on RA concrete to find its suitability for application in hot asphalt mixtures for urban paved roads. The study found that only asphalt pavements with 10% or 20% of CDW aggregate could be used as asphalt wearing courses of urban roads. Asphalt pavement with higher CDW aggregates tends to be more susceptible to moisture damage and plastic deformations. In a similar study, Herrador et al. [11] tried to verify the technical viability of using CDW aggregate as base pavement layers and road surfaces. Study found that CDW aggregate requires more water than natural aggregates. The load bearing capacity of the CDW aggregate was found to be satisfactory for application in the pavements. Gómez-Meijide and Pérez [12] studied Cold Asphalt Mixes (CAM) with 100% RA from CDW. The study suggests that traditional mix method may not be suitable for CAM production. Improvements in mechanical properties were found in CAM after production when NA are replaced by RA. CAM with RA shows better behavior under sudden moisture and temperature varying conditions.

There has been widely available literature [13–16] for the natural aggregate concrete. These studies include both the mechanical as well as fracture parameters. The studies in the literature also show some of the alternatives to these conventional natural aggregates [17] like fly ash sand as natural aggregate. Utilization of fly ash and other industrial waste for number of applications [18] has been widely studied in past. On similar grounds, for full scale implementation of RA from CDW into structural concrete and pavements, detailed insight into its mechanical and fracture properties becomes crucial. Fracture properties of concrete gives an indication of its brittleness as well as crack susceptibility and crack arresting capabilities. Choubey et al. [19] made an attempt to model the fracture parameter which affects the crack propagation in recycled aggregate based concrete. The paper applied the fictitious crack model and double-K fracture model to determine the fracture parameters of recycled aggregate based concrete with varying proportion of recycled aggregates. The peak load taken by the RA concrete reduced in both the models by 13% to 33% for RA replacement between 30% to 100%.

Wang et al. [20], studied coupling mechanism between freeze-thaw cycles and positive / negative effects of chemical phenomena such as chloride ion penetration, sulfate attack, carbonation, and alkali–silica reaction. Study highlighted that combined effect cannot be ignored as the combination of different degradation processes may be more severe than that of individual actions. Chemical mechanism can have both positive and negative effects on freeze thaw cycles, whereas physical actions such as external loading, salt crystallization, and wetting–drying cycles can aggravate freeze thaw damage. One major finding presented in study by Wang et al. [20] was that the degradation of physical and mechanical properties of concrete were related to type and dosage of chemical solution, as well as to load stress ratio. These physical and chemical damages to concrete can lead to changes in overall properties of construction and demolition waste aggregate. The resistance

of different concrete mixtures to combined action of F–T (Freeze-Thaw) cycles and sulfate attack was investigated by Li et al. [21]. Study indicated that resistance of low volume fly ash and high-volume fly ash based concrete mixtures to the combined effects of F–T cycles and sulfate attack increased along with the recycled aggregated based concrete content as replacement of natural aggregate based concrete. The resistance was more affected by FA content than by the replacement of natural and recycled aggregate based concrete. The sulfate solution produced a combined positive and negative effect on the concrete subjected to F–T cycle. The 5% sodium sulfate solution enhanced the concrete resistance to F–T cycle during the 300 F–T cycles, and the effect was similar both in low volume fly ash and high-volume fly ash-based concrete. Li et al. [22] used Scanning Electron Microscopy to investigate the morphology and average micro-crack width in (Interfacial Transition Zone) ITZ between the aggregate and the matrix of recycled aggregated based concrete after CO_2 curing, and the dependencies between the average micro-crack width in the ITZ area. Study discussed the mechanical properties of recycled aggregated based concrete and indicated a clear relationship between the mechanical properties of RAC and the average micro-crack width in the ITZ of recycled aggregate based concrete after CO_2 curing; wherein the mechanical properties of recycled aggregated based concrete (e.g., compressive strength and modulus of elasticity) increases with the decrease in average micro-crack width. García-Gonzalez et al. [23] evaluated fracture energy of recycled aggregate based concrete using wedge splitting test method and investigated the effect of water reducing admixture. Gain in compressive strength was observed by inclusion of water reducing admixture. Also, reduction in the fracture energy were reported when the percentage inclusion of recycled aggregate was more than 20%. Zheng et al. [24], studied the length and content of Basalt Fiber (BF), the concentration of Nano Silica (NS) solution, BF-reinforced recycled aggregate concrete containing NS-modified recycled aggregate based concrete, and micro-strengthening mechanism. They highlighted based on study that based on Scanning Electron Microscopy and Energy-dispersive Detector Spectroscopy (EDS) measuring, NS can effectively improve the pores and cracks of the internal structure of RA, reduce the calcium-silicon ratio of Interfacial Transition Zone (ITZ) between BF and cement matrix, and enhance the bonding of the ITZ. The rough surface of RA were beneficial to the distribution of BF, and the proper content of BF makes the spatial structure of RAC compact. Zheng et al. [25] studied the improvements in mechanical properties of RAC due to physical slurry removal, soaking in NS solutions with different concentrations for different amounts of time, and vibration stirring. Their study indicated that physical slurry removal, NS solution soaking, and vibration stirring reduced number of internal microcracks, increased density of the RAC, improved the structure of the ITZ, and improved the strength of the RAC. Zhang et al. [26] concluded through their study that inclusion of PVA fiber significantly improves fracture properties of the Polyvinyl-alcohol Fiber Reinforced Cementitious Composites (PVA-FRCC) under coupled effect of wet-thermal and chloride salt laden environment, and the improvement became more significant with increment in fiber dosage. With increase in PVA fiber dosage, peak load, initiation fracture toughness, unstable fracture toughness and fracture energy of PVA-FRCC increased gradually. In addition to effect of PVA fiber, such as anti-cracking and toughening, reason for the improvement of fracture performance may also be due to cement which may form new compounds in the early hydration reaction leading to pore refinement. Experimental study conducted by Zhang et al. [26, 27] highlighted that PVA fiber addition leads to improvement in the mechanical properties particularly compressive strength and fracture performance but decrease in workability was noticed. 0.8%–1.0% was considered as the optimum dosage of PVA fiber. Addition of 1% nano-SiO_2 shows a marginal improvement on both workability and mechanical properties of mortar irrespective of fiber content. Niu et al. [28] investigated the effect of municipal solid waste incineration fly ash (MFA) replacement ratios on basic mechanical properties and fracture performance of MFA-GPC (Geopolymer Concrete). The test results of their study indicated that mechanical properties of MFA-GPC decreased with increase of the MFA substitution ratio. Compared with controlled GPC without MFA, the maximum reduction rates of cubic compressive strength, splitting tensile strength, axial compressive strength, elastic modulus, initiation fracture toughness, unstable fracture toughness and fracture energy of MFA-GPC were 83%, 81%, 78%, 93%, 77%, 73% and 61%, respectively. Li et al. [29] conducted macroscopic and microscopic performance of early-age frost Roller Compacted Concrete (RCC) interface to investigate influence of pre-curing time and interval time on performance of RCC interface subjected to early-age frost damage. Study conducted by Li et al. [29] established the relationship between

macroscopic and microscopic performances of RCC interface that suffered early-age frost damage. They highlighted that shear strength increases with decrease in porosity and interfacial transition zone crack width. Study also concluded that increase in hydrostatic pressure were leading cause of damage in early-age frost RCC interface.

In present study, recycled aggregate (RA) from construction and demolition waste (CDW) has been used as a full substitute for natural coarse aggregate in the concrete. Beams having dimension of 100 mm × 100 mm × 500 mm were cast for comparing fracture performance of concrete made with recycled and natural aggregate. The specimens were tested as per RILEM's three-point bend test on notched beam and previous literature. The findings from the analysis for Recycled aggregate concrete has been compared with Natural aggregate concrete of similar strength range.

1.1 Research significance

The aim of study was to evaluate the fracture behavior of Recycled Aggregate based concrete using both experimental and Finite Element Method (FEM) analysis. Fracture parameters like fracture energy, stress intensity factor, energy release rate and characteristic length were evaluated from the Load-deflection and Load-CMOD (Crack Mouth Opening Displacement) curves for both concrete made with RA and natural aggregate. The FEM model have been used for simulating results from an experimental investigation conducted on beams with centric notches.

2 Materials and mix design

This section provides properties of the concrete making materials. The main materials include cement, fine aggregates, recycled coarse aggregate and super plasticizers. Cementitious materials include OPC 43 grade cement meeting the specifications of IS 269-2015. Physical and chemical properties of cement and fly ash used in the study were evaluated as per the Indian Standard code IS 4031, IS 4032 and IS: 1727 and results have been given in Table 1. The fineness of fly ash was 330 m^2/kg, specific gravity was 2.33 and lime reactivity was 4.35. Crushed sand conforming to Zone II as per IS 383-2016 has been used as fine aggregate in RA based concrete. The physical properties of fine and coarse aggregate were evaluated as per IS: 2386 and results are tabulated in Table 2. Recycled aggregates obtained from construction and demolition waste have been used in study and its physical properties has been given in Table 2. For both mixes, Polycarboxylic group-based superplasticizer has been used.

Table 1 Properties of cement

Characteristics	OPC-43	Fly ash
Physical Tests		-
Fineness (m^2/kg)	271.00	-
Soundness (Autoclave) (%)	00.05	-
Soundness (Le Chatelier's) (mm)	1.5	-
Setting Time Initial & Final (min.)	130.00 and 180.00	-
Specific gravity	3.15	-
Chemical Tests		
Loss of Ignition (LOI) (%)	3.23	4.76
Silica (SiO_2) (%)	20.19	48.66
Iron Oxide (Fe_2O_3) (%)	4.39	8.87
Aluminium Oxide (Al_2O_3)	4.97	26.72
Calcium Oxide (CaO) (%)	61.84	5.80
Magnesium Oxide (MgO) (%)	1.83	1.43
Sulphate (SO_3) (%)	2.08	0.75
Na_2Oeq (%)	0.61	0.74
Chloride (Cl) (%)	0.018	0.026
IR (%)	1.64	-

Table 2 Properties of recycled coarse aggregates and natural fine aggregates

Property		Recycled Coarse aggregates		Fine Aggregate (Natural)
		20 mm	10 mm	
Specific gravity		2.39	2.37	2.64
Water absorption (%)		4.58	4.75	0.8
Soundness test (Na_2SO_4)		0.13	-	-
Aggregate Abrasion value %		24	22	-
Aggregate Crushing Value %		25	26	-
Aggregate Impact Value %		20	17	-
Combined flakiness and Elongation Index %		15.8	20	-
Total Deleterious material (%)		0.1	0.1	0.5
Sieve Analysis Cumulative Percentage Passing (%)	40 mm	100	100	100
	20mm	93	100	100
	10 mm	2	74	100
	4.75 mm	1	6	95
	2.36 mm	0	0	87
	1.18 mm	0	0	68
	600 µ	0	0	38
	300 µ	0	0	10
	150 µ	0	0	2
	Pan	0	0	0

Optical microphotographs of petrography study done for aggregated used in study of Ojha et al. [17] has been given in Fig. 1 and discussed in subsequent lines. The type of coarse aggregates used were granite. The major mineral constituents were quartz, biotite, plagioclase feldspar and orthoclase-feldspar. Accessory minerals were calcite, muscovite, tourmaline, and iron oxide. Grain size of quartz were from 3 µm to 307 µm with an average of 167 µm. Majority of quartz grains were in size range of 140 µm to 170 µm. The strained quartz percentage was about 19% and Undulatory Extinction Angle (UEA) varied from 15° to 17°. The petrographic analysis of recycled aggregates were not conducted due to wide variation in types of aggregates as seen through visual examination. The impact, crushing and abrasion values of natural granite coarse aggregate were 13%, 19% and 19%, respectively. The impact, crushing and abrasion values of recycled coarse aggregate were 25%, 20% and 24%, respectively. Adhered mortar surrounding the natural aggregate in RCA were porous in nature. Due to the soft nature of adhered mortar, use of RCA becomes problematic and restricts the application of RCA in the concrete production. Therefore, it becomes necessary to remove this layer as much as possible. In case of properties like specific gravity and water absorption value, a significant improvement has been observed in mechanically treated aggregate after 500 revolutions in LOS Angeles machine which supports removal of the adhere mortar. The percentage increase in specific gravity was found in the range of 1.27% to 7.17% for 10 mm aggregate and for 20 mm aggregate, percentage increase in specific gravity was observed as 1.26% for recycled coarse aggregates obtained from construction and demolition aggregate Plant in Burari, Delhi-India. The percentage reduction in the water absorption was found in the range of 3.39% to 17.26%, for 10 mm aggregate and for 20 mm aggregate, percentage reduction in water absorption was observed as 15.50% RCA generated from Burari plant.

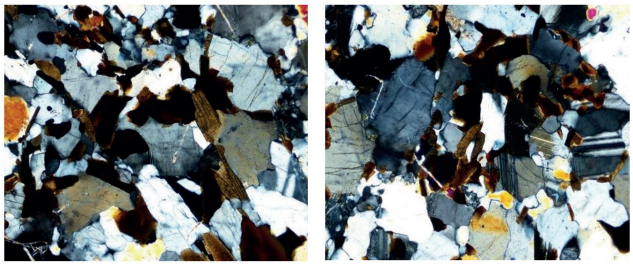

Fig. 1 Shows distribution of quartz, biotite, plagioclase-feldspar, orthoclase-feldspar, calcite, muscovite, and iron oxide grains in sample (5x, X-Nicols)

The details of concrete mixes have been given in Table 3. Two concrete mixes 0.4_RA and 0.5_RA represents the concrete with 100% recycled coarse aggregate having w/b ratio as 0.4 and 0.5, respectively. One concrete mix 0.47_RA represents the concrete with 100% natural coarse aggregate and w/b ratio of 0.47. The study has been used to compare the fracture parameters of natural and recycled aggregates.

3 Experimental setup and procedure

In this section, studies on compressive strength, split tensile strength, modulus of elasticity, Poisson's ratio and 3-Point bend test on notched beams have been discussed. Findings and derivation of other parameters related to these tests have been further explained in result and discussion section of the manuscript.

3.1 Mechanical properties of concrete

The compressive strengths of specimens were analyzed and recorded at 28 days age as per IS: 516. The tensile strength test was carried out on cylindrical concrete specimens and results were determined as per IS: 5816-1999 over the curing period of 28 days. Modulus of elasticity and Poisson's ratio of samples has been evaluated using ASTMC-469 [30]. Average value of set of three specimens for each of these tests had been used.

3.2 Three-point bend test on notched beam

Various fracture parameters were evaluated for a notched beam specimen using the test method of 3-Point bend test proposed by RILEM [29, 31]. A schematic diagram representing the 3-Point bend test and the laboratory setup used has been shown in Fig. 2. Accordingly, notched beams

Table 3 Mix design details

Mix Parameter	0.4_RA	0.5_RA	0.47_NA
OPC (kg/m^3)	380	350	290
Fly ash (kg/m^3)	-	-	72
w/b	0.4	0.5	0.47
Water (kg/m^3)	152	175	152
Fine Aggregate (kg/m^3)	726	660	650
Coarse Aggregate 10 mm, (kg/m^3)	730	775	777
Coarse Aggregate 20 mm, (kg/m^3)	487	520	518
Admixture % by weight of cement	0.40	0.35	0.40
Mix ID 0.4_RA represents the concrete with 100% recycled coarse aggregate and w/b ratio of 0.40			
Mix ID 0.5_RA represents the concrete with 100% recycled coarse aggregate and w/b ratio of 0.50			
Mix ID 0.47_NA represents the concrete with 100% natural coarse aggregate and w/b ratio of 0.47			

with a notch of 35 mm at the mid span and dimension of 100 mm × 100 mm × 500 mm were prepared with a clear span of 400 mm as shown in Fig. 3. In order to maintain the continuous stability of test, the disc spring reinforcement device of test equipment was used to strengthen the testing equipment. The load sensor was used to measure the load of the notched three-point bending beam, and the measuring range of the sensor was 0–30 kN (Fig. 4). In order to remove the influence of bearing deformation on the deflection test results, deflection test beam was arranged directly above the support point of the three-point bending specimen, and the mid-span deflection is measured with a Linear Variable Displacement Transducer (LVDT). The Crack Mouth Opening Displacement (CMOD) clip extensometer was arranged at the bottom of the beam with a 3 mm thick alloy aluminum knife edge. The crack tip opening displacement clip extensometer was fixed at the tip of the crack on the side of the beam with a knife edge. This study was based on the displacement-controlled test in which the load application leads to a constant increase in CMOD values (0.40 μ/s) and the test was carried out till the failure of beam. The continuous loading mode was adopted in during test, and the computer data acquisition system was used to obtain the automatic data acquisition. The load deflection curve and load-CMOD (P-CMOD) curve was recorded simultaneously.

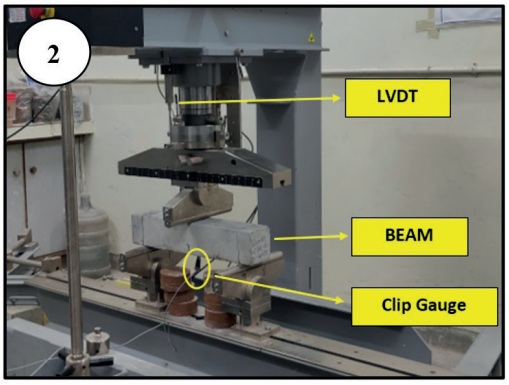

Fig. 2 Setup for three-point bend test

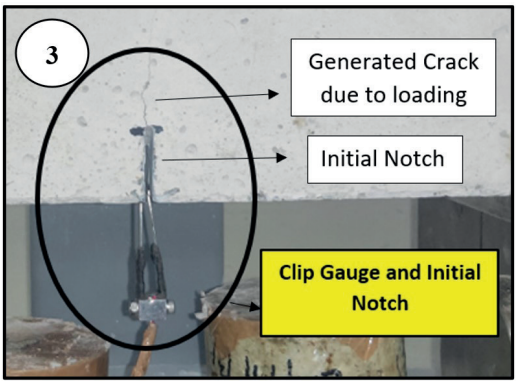

Fig. 3 Initial notch, generated crack due to loading and clip gauge measuring CMOD

4 FEM modelling and analysis

A simple geometry for studying non-planar fracture in RCA based concrete and normal aggregate based concrete adopted in the study was the centric notched beam under three-point bend test. Such type of specimen has been adopted in past by other researchers also to study the mixed mode fracture [29–34]. FEM analysis was performed using ANSYS workbench program [35]. Models for the beam were created and various fracture parameters were evaluated. For simulating the experimentation in FEM analysis, beam size was adopted similar to the beam size used in experimentation. The un-cracked part is represented with triangular and quadrilateral finite elements, and the crack path by interface elements. For non-planar cases, average crack paths obtained from the experimental bands were used while in mode I the crack path has been taken to be straight. The computations were made with quadratic analysis, using Gauss 3 × 3 integration rule in quadrilateral elements and the 7-point Gauss rule in triangular elements and 3-point Newton–Cotes rule in interfaces. The choice of integration rule for interface element were important since Gauss rule leads to results with spurious jumps in strain and stress fields. In order to obtain stable results after the

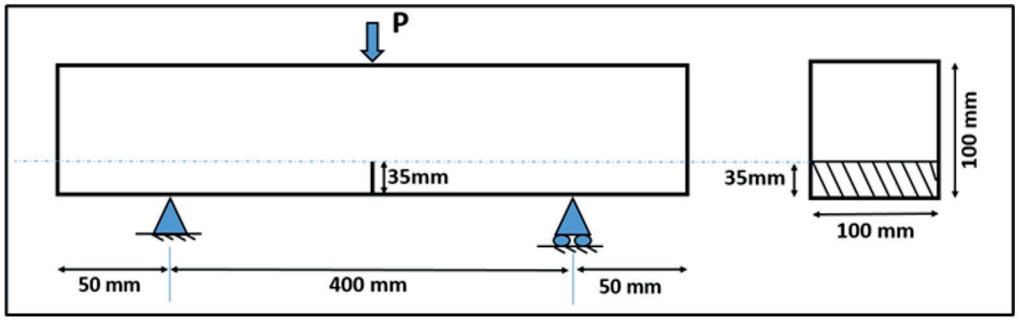

Fig. 4 Beam dimensions and notch depth for the test [26]

peak load, a displacement control method were used for increasing the CMOD monotonically and calculations take into account the weight of the concrete. Fig. 5(a) shows the front view of beam. The beam was supported using two supports S1 and S2 as shown in Fig. 5(b) at S1 displacement in both the y and x directions were restrained and at S2, only the displacement in y direction was restrained. This created a simply supported system. Fig. 5(c) shows the loading arrangement. Maximum load based on the experimental maximum load taken by the beam has been applied at L1 as shown in Fig. 5(c). The width of surface S1, S2 and S3 was taken as 2 mm to avoid the stress concentration on line. The model consists of 623101 nodes and 590200 elements. The element adopted for the study was solid185. In addition, traditional node-to-surface discretization, as well as the approach of the small sliding tracking has been adopted similar to study by Altheeb et al. [36] to model interaction, which resulted from mortar located amid the block units. The interaction properties in this study were modeled via a normal behavior as a hard contact (i.e., no penetration of surfaces) and a tangential behavior by specifying the friction coefficients between the steel and concrete surfaces as 0.47 [37]. Efforts on the refinement of the mesh did not result in better convergence from Mesh and required longer running time and more resources [38–40]. Minimum element size for the beam was adopted as 5 mm but for notch tip element size of 0.5 mm was adopted as can be seen in Fig. 5(a). The material properties for the beam are similar to the properties evaluated experimentally and presented above.

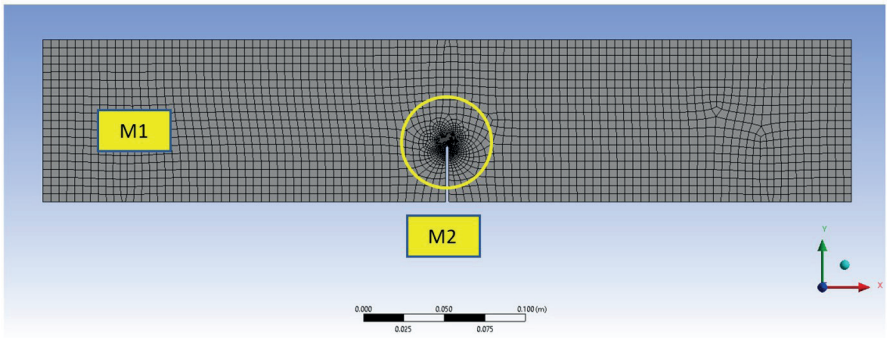

(a)

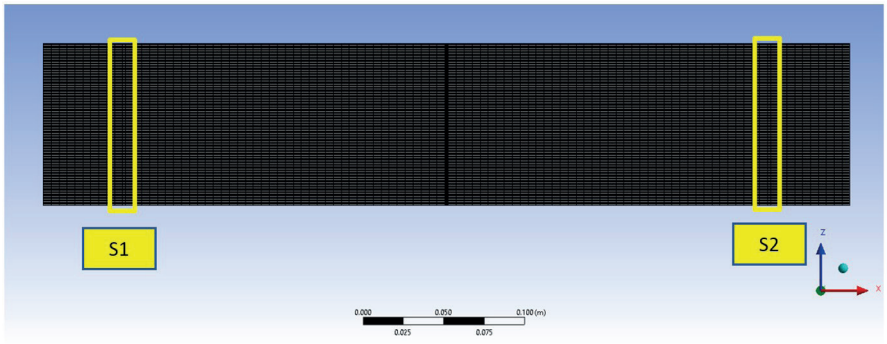

(b)

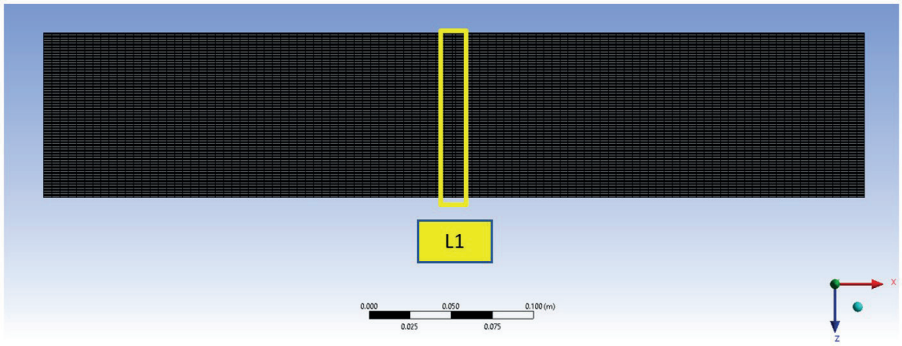

(c)

Fig. 5 (a) Meshed beam showing notch- front view, (b) Meshed beam showing supports-bottom view, (c) Meshed beam showing loading surface – top view

5 Results and discussions

The section presents the findings from the experimental as well as the FEM analysis.

5.1 Mechanical properties of concrete

The compressive strength, split tensile strength, modulus of elasticity [41] and Poisson's ratio has been shown in Table 5.

Density of the concrete mix with recycled aggregate were lower than density of conventional aggregate concrete. This can be attributed to the higher density of the natural aggregate. Concrete made with recycled aggregate with w/b ratio of 0.5 has lowest compressive strength of 29.3 MPa and concrete made with natural aggregate and w/b ratio of 0.47 has the highest compressive strength. The Modulus of Elasticity (MOE) values were highest for 0.4_RA sample and lowest for 0.47_NA sample. The old adhered mortar in Recycled Aggregate based concrete which causes reduction in compressive strength leading to weak ITZ was removed by mechanical action in Los-Angeles abrasion equipment. The values are used as an input parameter to model material behavior in FEM. The Poisson's ratio, defined as ratio of transverse strain and longitudinal strain was comparable for both RA and natural aggregate based concrete. The values of Poisson's ratio vary from 0.15 to 0.17 for all the mixes. The split tensile strength was about 10% of compressive strength in cases of both RA and natural aggregate based concrete depicting similar trend with respect to ratio of split tensile to compressive strength of concrete.

5.2 Load-CMOD and load-deflection curves

Fig. 6 shows, Load-CMOD and Load-deflection curves for different mixes considered in the study. The figure in case of 0.5_RA and 0.4_RA beams shows sudden collapse at the peak load without showing any gradual declining limb. The figure in case of beams with concrete made of natural aggregate shows mix failure with gradual failure after the peak load in few cases and sudden failure after the peak load in few cases. Also, the curves for the RCA shows a slightly higher peak load during the three-point bend test than a natural aggregate based mix. The rising limb of both the RCA based mixes were less steep than the natural aggregate based concrete in the load deformation curves. From load deflection curves in Fig. 6, it can be observed that there was increase in the deflection at peak stress for RCA based mixes as compared to the natural aggregate based concrete. The peak stress increased and the ascending branch was less steep and descending part of load deflection curves were steep for RCA based concrete. Whereas for natural aggregate based concrete both ascending branch and descending part of the load deflection curves were steep and peak stress was slightly lower than peak stress of RCA based concrete.

With increase in load, deformation of concrete specimen attains initial crack strain and concrete matrix starts to show some micro-cracks and subsequently the load deflection curve starts to show a non-linear growth. With development of macroscopic cracks, the cracks in matrix concrete continue to grow and both RCA based concrete & natural aggregate based concrete reaches in its elastic-plastic stage. The pattern of experimentally obtained curves of load–crack mouth opening displacement (CMOD) are quite similar for both RCA based concrete and natural aggregate based concrete. But the peak load was lower in case of natural aggregate based concrete as compared to RCA based concrete similar to the trend noticed in Load-deflection curves which indicates effect of aggregate properties on the tensile load and CMOD properties concrete.

5.3 Results from the FEM analysis

The average maximum load taken by the beams in each of the mixes has been applied on the beam for the numerical simulation of the stresses and the deformation at the nodes in the beam. Fig. 7 shows the Von-Mises Stress and Fig. 8 shows the deformation of the nodes in the modelled beam for three different concrete mixes adopted in this study. The maximum stress was observed in the beam with mix ID 0.5_RA. The reason can be attributed to the highest peak load depicted by the mix in three-point bend test.

Table 5 Compressive strength, split tensile strength, M.O.E. and Poisson's ratio

	0.4_RA	0.5_RA	0.47_NA [36]
Density (kg m^{-3})	2323.054 σ = ±60	2338.352 σ = ±75	2433.02 σ = ±70
M.O.E. (MPa)	34294 σ = ±150	31874 σ = ±175	29520 σ = ±160
Poisson's ratio	0.16	0.15	0.17
Split tensile strength (MPa)	3.25 σ = ±0.25	2.8 σ = ±0.2	3.37 σ = ±0.30
Compressive strength (MPa)	39.09 σ = ±4.5	29.3 σ = ±3.5	36.9 σ = ±3.75

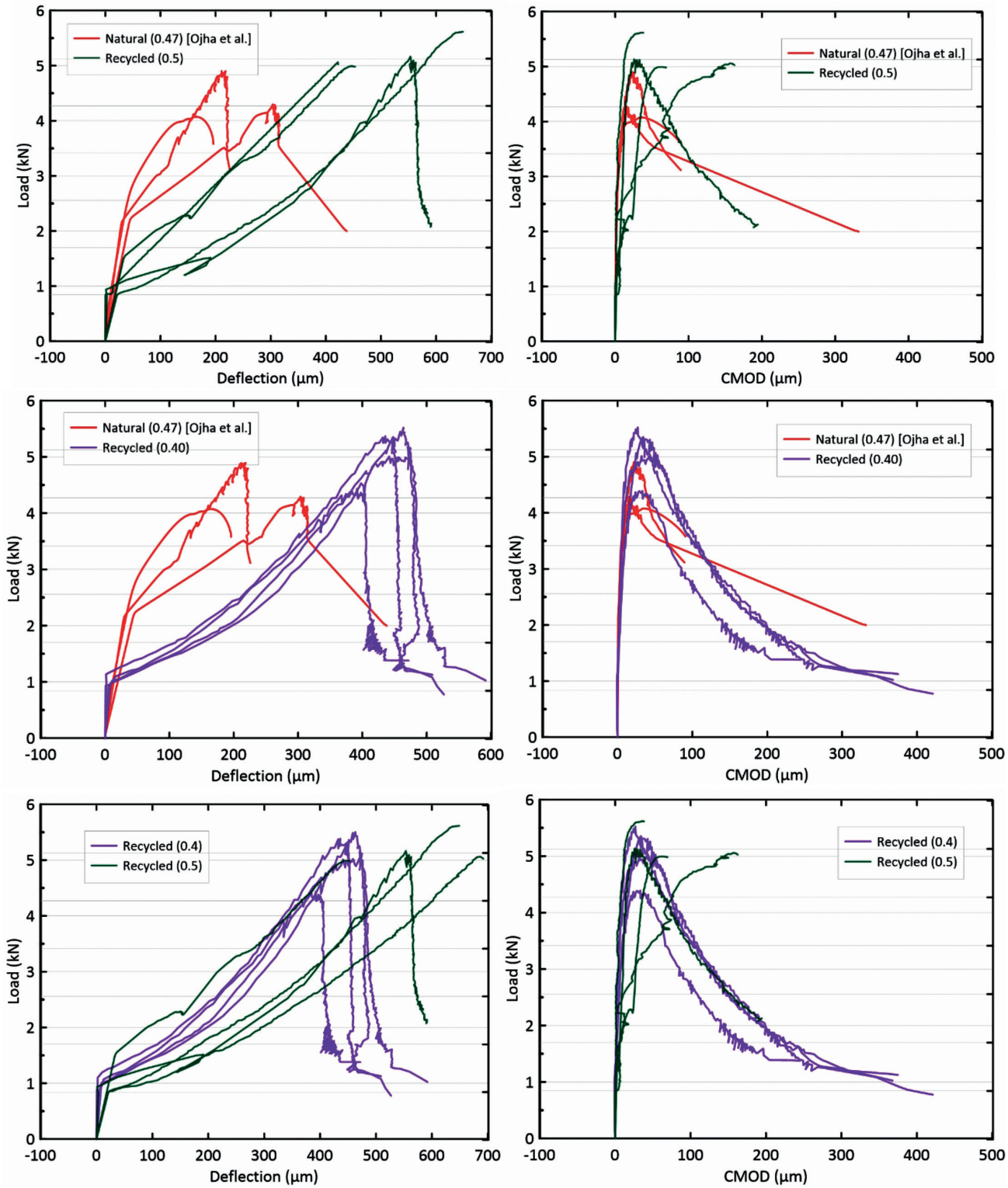

Fig. 6 Load-CMOD and load-deflection curves

The maximum deformation has been observed in concrete with natural aggregate studied by Ojha et al. [37]. Apart from the stresses and deformation at nodes, a number of other fracture parameters were evaluated for the concrete beams. This includes maximum stress intensity for three modes of fracture (K1, K2 and K3), average energy release rate by VCCT (Virtual Crack-Closure Technique) method and the J-Integral. The values of fracture parameters obtained from FEM analysis of the beams has been tabulated in Table 6.

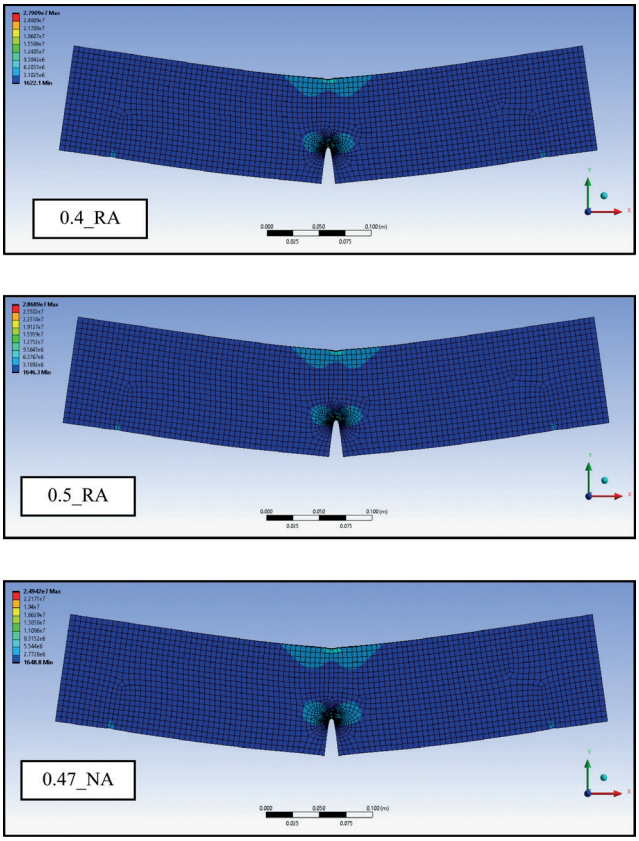

Fig. 7 Meshed beam showing von Mises stresses in the beam

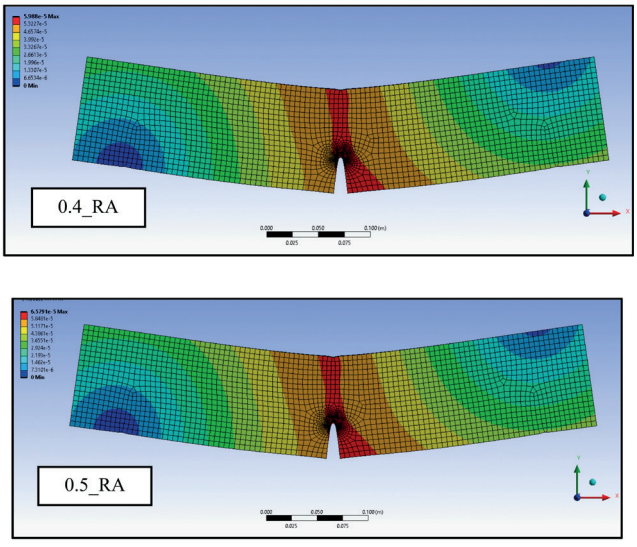

Fig. 8 Meshed beam showing deformation in the beam

The load deflection curves were compared with the input value. The direct application of cohesion produced results that were smaller than true value, while the proposed method of applying cohesion by the element solid 185 can improve the accuracy of the applied cohesion. The difference in numerical results show that applying cohesion is necessary for numerical simulation, and accuracy of cohesion can influence results of numerical simulation. The method can be applicable to numerical simulation for the concrete mode I crack propagation process by improving accuracy of cohesion applied on concrete fracture process zone [39]. According to crack propagation criterion based on initial fracture toughness, more numerical simulations may be needed to explore the effect of cohesion application in modes I crack propagation process, which needs further study. The equivalent von-Mises stresses as shown in Fig. 7 are higher in cases recycled aggregate based concrete for both water to cement ration of 0.4 and 0.5 as compared to natural aggregate based concrete with water to cement ratio of 0.47. The total deformation as shown in Fig. 7 were less in cases recycled aggregate based concrete for both water to cement ration of 0.4 and 0.5 as compared to natural aggregate based concrete with water to cement ratio of 0.47. The fracture energy parameter for stress intensity factor obtained through FEM analysis were similar to experimental results wherein no significant variation in stress intensity factor between all the three concrete mixes was observed. However, it can be stated that values of stress intensity factor of 0.47_NA was the lowest and 0.5_RA was the highest. The fact that the analytical results did not exactly match with experimental results can be attributed to inability to actual notch dimensions, crack paths and boundary conditions in the modelling but trends were similar to experimental results.

Table 6 Fracture parameters obtained from FEM analysis

	0.4_RA	0.5_RA	0.47_NA
K1 (MPa√m)	1.1013	1.123	1.0669
K2 (Pa√m)	57.562	59.441	55.496
K3 (Pa√m)	44.898	44.489	55.257
G1 (N/m)	22.46	25.193	23.91
G2 (N/m)	2.1735e-3	2.529e-3	1.3685e-3
G3 (N/m)	1.0627e-6	1.1158e-6	1.9622e-6
GT (N/m)	22.463	25.196	23.912
J-Integeral (N/m)	35.613	39.926	38.136

5.4 Fracture energy

One of the basic properties of the material which can be useful in analyzing and determining crack resistance, brittleness and toughness can be termed as fracture energy (G_f) which is defined as the energy required to create a unit crack in a given specimen [32]. This energy can be calculated using Eq. (1).

$$G_f\left(N/m\right)=\left(W_o+mg\delta_o\right)/A_{lig} \tag{1}$$

The above equation for calculating G_f uses W_o as the area under the load-deflection curve for the tested beam, g is acceleration due to gravity, i.e., 9.81 m/s^2, m as total weight which includes total weight of loading arrangement not attached to beam and total weight of beam between supports, A_{lig} as area of ligament representing area of projection of fractural zone on plane perpendicular to axis of beam. Fig. 9 shows comparative plots for different mixes considered. From the plots, it is evident that there were no significant difference in average fracture energy of the mixes and it lies in range of 180 N/m to 300 N/m.

Natural aggregate based concrete with w/b ratio of 0.47 shows lower fracture energy. Among recycled aggregate based concrete, concrete mix having w/b ratio of 0.5 show a relatively better fracture energy. The better fracture energy of RA concrete can be attributed to the removal of adhered mortar by mechanical treatment leading to reduction of the width and length of cracks in old ITZ and reduction of pore size of adhered mortar which ultimately improves bond between RCA and new cement paste. This resulted in better ITZ for RA based concrete along with better resistance to crack propagation. The specimen reinforced with hybrid 0.1% PP-0.9% steel fiber-reinforced rubberized concrete, produced higher levels of fracture energy of approximately 3716.6 N/m which is 13 times higher than that of plain concrete. Addition of fibers causes bridging action and thereby improving fracture performance in concrete with fiber as compared to plain concrete containing both recycled and natural aggregate based concrete [32, 38–42]. With the addition of fiber, crack development path becomes relatively tortuous, from single crack propagation of reference group to multi-point cracking of more than one crack, and with increase of VF, crack propagation path becomes more tortuous.

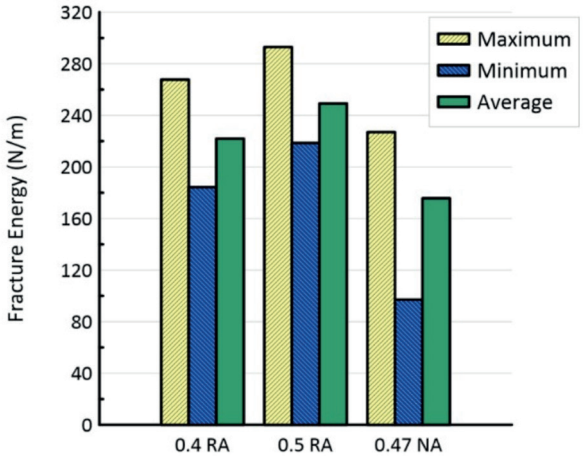

Fig. 9 Experimental value of fracture energy

5.5 Stress intensity factor

Stress Intensity Factor (K_{IC}) is a factor which quantifies the stress in the surrounding of a crack and is useful in comparing the brittleness of two separate materials. As the values of KIC increases the ability of concrete to bear higher stresses around the crack increases showing less brittle behavior. This factor can be calculated using the following Eq. (2) as given in RILEM TC 89-FMT [31]:

$$K_{IC}\left(MPa\sqrt{m}\right)=3\left(P_{N\max}+0.5mg\right)\frac{S\sqrt{\pi a}}{2d^2b}f\left(\alpha\right). \quad (2)$$

In the above equation, S is span of the beam in m, α is ratio of a and d i.e., $\alpha = a/d = 0.35$, $P_{N\max}$ is given as maximum load that is applied on the notched prism in Newton and $f(\alpha)$ is used for geometry correction for bending load and is given by Eq. (3) as follows:

$$f\left(\alpha\right)=\frac{1.99-\alpha\left(1-\alpha\right)\left(2.15-3.9\alpha+2.7\alpha^2\right)}{\sqrt{\pi}\left(1+2\alpha\right)\left(1-\alpha\right)^{3/2}}. \quad (3)$$

The comparison of values for the stress intensity factor has been shown in Fig. 10. Similar to fracture energy, no significant variation in stress intensity factor between three concrete mixes was observed. However, it can be stated that values of stress intensity factor of 0.47_NA was the lowest and 0.5_RA was the highest. This suggests that the mix with recycled aggregate having w/b ratio of 0.5 can take larger stresses around the crack. Improvement in aggregate surface characteristics due to mechanical treatment of RA led to enhancement in bond between cement paste aggregate interface thereby allowing specimens made with recycled aggregate to take a higher stress at fracture tip resulting in improved stress intensity factor.

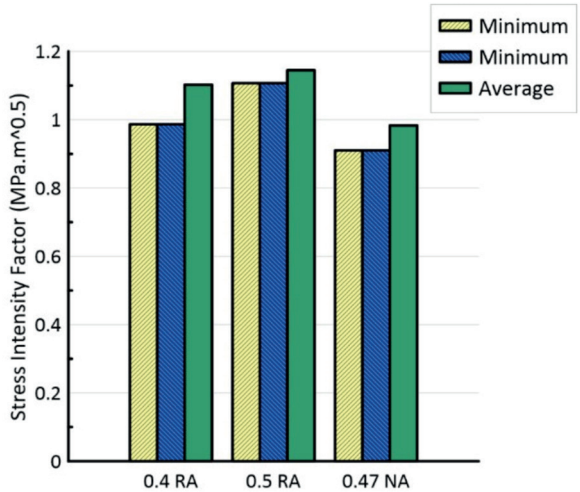

Fig. 10 Experimental value of Stress Intensity Factor

5.6 Characteristic length

In nonlocal continuum formulations, characteristic length is a material parameter that indicates the smallest possible breadth of a zone of strain-softening damage [33]. In discrete fracture models, it may be thought of as the smallest feasible fracture length. Characteristic length is a measure of brittleness of materials in terms of the beginning of early fractures. Materials having smaller characteristic length are more brittle. Therefore, fracture propagation is easier in case of such materials. It can be evaluated using Eq. (4) based on literature [34] as given below.

$$L_{ch}\left(mm\right)=\frac{EG_f}{f_{st}^{\ 2}} \tag{4}$$

In Eq. (4) E is the young's modulus, G_f is the fracture energy and f_{st} is the split tensile strength for the mix. The calculated values for the energy release rate is presented in Fig. 11. On average, all the mix have similar characteristic length, indicating that degree of brittleness were similar when comparison was based on characteristic length criteria.

5.7 Energy Release rate

The energy release rate is the rate at which energy is changed as a material fractures and a new surface emerges. It is expressed quantitatively as the reduction in total potential energy per unit increase in fracture surface area. The energy release rate is a critical component in determining material properties linked to fracture and fatigue. It can be evaluated using Eq. (5) as presented in literature [35–36].

$$G_{IC}\left(\frac{N}{m}\right)=\frac{K_{IC}^{\ 2}}{E} \tag{5}$$

In Eq. (5), KIC is stress intensity factor and E is the modulus of elasticity of the specimen. The comparative graphs for the energy release rate has been shown in Fig. 12. The graph shows the highest energy release rate in case of 0.5_RA and lowest in case of 0.47_NA. Therefore, the recycles aggregate based concrete has a superior fracture performance than the natural aggregate concrete in terms of energy release rate. Similar to fracture energy, owing to a better ITZ formation in RA based concrete which leads to fracture energy being slightly better than the fracture energy of NA based concrete.

6 Conclusions

The study presents an experimental investigation and FEM analysis of the fracture performance of concrete made using Construction and Demolition based recycled aggregate. The study also compares the behavior of RCA based concrete with natural aggregate based concrete. Based on the study, following conclusions can be derived:

- The Modulus of Elasticity values were highest for 0.4_RA sample and lowest for 0.47_NA sample. The old adhered mortar in Recycled Aggregate based concrete which causes reduction in compressive strength leading to weak interfacial transition zone was removed by mechanical action in Los-Angeles abrasion equipment. The split tensile strength is about 10 percent of compressive strength in cases of both RA based concrete and natural aggregate based concrete depicting similar trend with respect to ratio of split tensile strength to compressive strength of concrete.
- There has been increase in the deflection at peak stress for RCA based concrete mixes as compared to the natural aggregate based concrete. The peak stress increased and the ascending branch was less

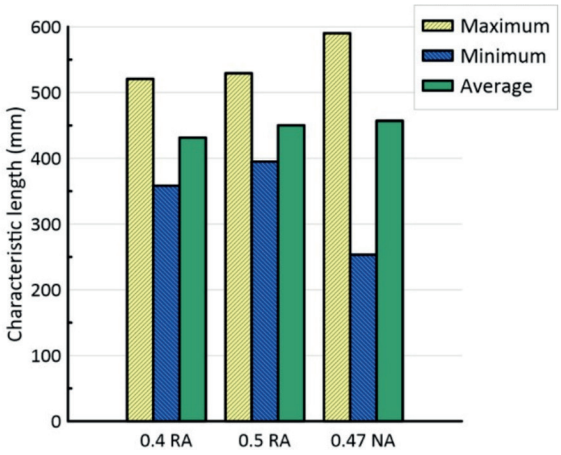

Fig. 11 Experimental value of characteristic length

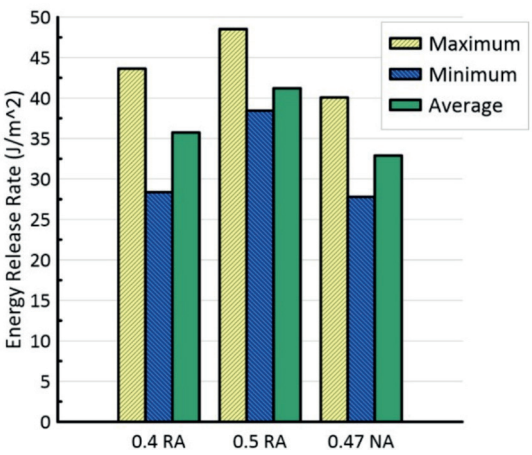

Fig. 12 Experimental value of energy release rate

steep and descending part of the load deflection curves were steep for RCA based concrete. The pattern of experimentally obtained curves of load Crack Mouth Opening Displacement (CMOD) were quite similar for both RCA and natural aggregate based concrete. But the peak load was lower in case of natural aggregate based concrete as compared to RCA based concrete

- Comparison of the fracture parameters for NCA concrete and RCA concrete suggests that the fracture performance of RCA concrete was slightly better than NCA concrete in terms of fracture energy, stress intensity factor, energy release rate and characteristic length. The fracture energy parameter in terms of stress intensity factor obtained through FEM analysis was similar to experimental results wherein no significant variation in stress intensity factor between the three concrete mixes was observed. However, it can be stated that values of stress intensity factor of 0.47_NA was lowest and 0.5_RA was highest. There is no significant difference in average fracture energy of mixes and it lies in range of 180 N/m to 300 N/m.
- The difference in numerical results show that applying cohesion was necessary for numerical simulation, and accuracy of cohesion can influence results of numerical simulation. According to crack propagation criterion based on initial fracture toughness, more numerical simulations may be needed to explore the effect of cohesion application in modes I crack propagation process, which needs further study.
- The fracture performance of RA concrete can be attributed to processing on RA in which removal of adhered mortar by mechanical treatment was done which reduced the width and length of cracks in old ITZ and pore size of attached mortar as well enhancement in bond between RCA and new cement paste. This resulted in better ITZ for RA concrete along with better resistance to crack propagation.

References

[1] Ojha, P. N., Arora, V. V., Trivedi, A., Singh, A., Singh, B., Kaushik, N. "Experimental Investigations on Use of C&D Waste as an Alternative to Natural Aggregates in Concrete", 4(1), pp. 58–70, 2021.
https://doi.org/10.26392/SSM.2021.04.01.058

[2] Silva, R. V., de Brito, J., Dhir, R. K. "Properties and composition of recycled aggregates from construction and demolition waste suitable for concrete production", Construction and Building Materials, 65, pp. 201–217, 2014.
https://doi.org/10.1016/j.conbuildmat.2014.04.117

[3] Wagih, A. M., El-Karmoty, H. Z., Ebid, M., Okba, S. H. "Recycled construction and demolition concrete waste as aggregate for structural concrete", HBRC Journal, 9(3), pp. 193–200, 2013.
https://doi.org/10.1016/j.hbrcj.2013.08.007

[4] Rao, A., Jha, K. N., Misra, S. "Use of aggregates from recycled construction and demolition waste in concrete", Resources, Conservation and Recycling, 50(1), pp. 71–81, 2007.
https://doi.org/10.1016/j.resconrec.2006.05.010

[5] Martín-Morales, M., Zamorano, M., Ruiz-Moyano, A., Valverde-Espinosa, I. "Characterization of recycled aggregates construction and demolition waste for concrete production following the Spanish Structural Concrete Code EHE-08", Construction and Building Materials, 25(2), pp. 742–748, 2011.
https://doi.org/10.1016/j.conbuildmat.2010.07.012

[6] Alexandridou, C., Angelopoulos, G. N., Coutelieris, F. A. "Mechanical and durability performance of concrete produced with recycled aggregates from Greek construction and demolition waste plants", Journal of Cleaner Production, 176, pp. 745–757, 2018.
https://doi.org/10.1016/j.jclepro.2017.12.081

[7] Bravo, M., Silva, A. S., de Brito, J., Evangelista, L. "Microstructure of Concrete with Aggregates from Construction and Demolition Waste Recycling Plants", Microscopy and Microanalysis, 22(1), pp. 149–167, 2015.
https://doi.org/10.1017/s1431927615015512

[8] Ahmed, S. F. U. "Properties of Concrete Containing Construction and Demolition Wastes and Fly Ash", Journal of Materials in Civil Engineering, 25(12), pp. 1864–1870, 2013.
https://doi.org/10.1061/(asce)mt.1943-5533.0000763

[9] Angulo, S. C., Carrijo, P. M., Figueiredo, A. D., Chaves, A. P., John, V. M. "On the classification of mixed construction and demolition waste aggregate by porosity and its impact on the mechanical performance of concrete", Materials and Structures, 43, pp. 519–528, 2010.
https://doi.org/10.1617/s11527-009-9508-9

[10] Ossa, A., Garcia, J. L., Botero, E. "Use of recycled construction and demolition waste (CDW) aggregates: A sustainable alternative for the pavement construction industry", Journal of Cleaner Production, 135, pp. 379–386, 2016.
https://doi.org/10.1016/j.jclepro.2016.06.088

[11] Herrador, R., Pérez, P., Garach, L., Ordóñez, J. "Use of Recycled Construction and Demolition Waste Aggregate for Road Course Surfacing", Journal of Transportation Engineering, 138(2), pp. 182–190, 2012.
https://doi.org/10.1061/(asce)te.1943-5436.0000320

[12] Gómez-Meijide, B., Pérez, I. "Effects of the use of construction and demolition waste aggregates in cold asphalt mixtures", Construction and Building Materials, 51, pp. 267–277, 2014.
https://doi.org/10.1016/j.conbuildmat.2013.10.096

[13] Singh, B., Arora, V. V., Patel, V. "Study on stress strain characteristics of high strength concrete", Indian Concrete Journal, 92(6), pp. 37–43, 2018.

[14] Singh, B., Arora, V. V., Patel, V. "Experimental study on stress strain behaviour of normal and high strength unconfined concrete", Indian Concrete Journal, 94(4), pp. 10–19, 2020.

[15] Arora, V. V., Singh, B., Patel, V., Trivedi, A. "Evaluation of modulus of elasticity for normal and high strength concrete with granite and calc-granulite aggregate", Structural Concrete, 22(S1), pp. E143-E151, 2021.
https://doi.org/10.1002/suco.202000023

[16] Patel, V., Singh, B., Arora, V. V. "Study on fracture behaviour of high strength concrete including effect of steel fiber", Indian Concrete Journal, 94(4), pp. 1–9, 2020.

[17] Ojha, P. N., Singh, B., Kaura, P., Singh, A. "Lightweight geopolymer fly ash sand: an alternative to fine aggregate for concrete production", Research on Engineering Structures and Materials, 7(3), pp. 375–391, 2021.
https://doi.org/10.17515/resm2021.257ma0205

[18] Singh, B., Ojha, P. N., Trivedi, A., Patel, V., Arora, V. V. "Development of Empirical Equations for Prediction of Flexural and Split Tensile Strength for Normal and High Strength Concrete with Granite and Calc-Granulite Aggregate", Indian Concrete Journal, 95(11), pp. 36–46, 2021.

[19] Choubey, R. K., Kumar, S., Chakradhara Rao, M. "Modeling of fracture parameters for crack propagation in recycled aggregate concrete", Construction and Building Materials, 106, pp. 168–178, 2016.
https://doi.org/10.1016/j.conbuildmat.2015.12.101

[20] Wang, R., Zhang, Q., Li, Y. "Deterioration of concrete under the coupling effects of freeze–thaw cycles and other actions: A review", Construction and Building Materials, 319, 126045, 2022.
https://doi.org/10.1016/j.conbuildmat.2021.126045

[21] Li, Y., Wang, R., Li, S., Zhao, Y., Qin, Y. "Resistance of recycled aggregate concrete containing low- and high-volume fly ash against the combined action of freeze–thaw cycles and sulfate attack", Construction and Building Materials, 166, pp. 23–34, 2018.
https://doi.org/10.1016/j.conbuildmat.2018.01.084

[22] Li, Y., Fu, T., Wang, R., Li, Y. "An assessment of microcracks in the interfacial transition zone of recycled concrete aggregates cured by CO2", Construction and Building Materials, 236, 117543, 2020.
https://doi.org/10.1016/j.conbuildmat.2019.117543

[23] García-González, J., Barroqueiro, T., Evangelista, L., de Brito, J., De Belie, N., Morán-del Pozo, J., Juan-Valdés, A. "Fracture energy of coarse recycled aggregate concrete using the wedge splitting test method: influence of water-reducing admixtures", Materials and Structures, 50, 120, 2017.
https://doi.org/10.1617/s11527-016-0989-z

[24] Zheng, Y., Zhuo, J., Zhang, Y., Zhang, P. "Mechanical properties and microstructure of nano-SiO2 and basalt-fiber-reinforced recycled aggregate concrete", Nanotechnology Reviews, 11(1), pp. 2169–2189, 2022.
https://doi.org/10.1515/ntrev-2022-0134

[25] Zheng, Y., Zhang, Y., Zhuo, J., Zhang, P., Kong, W. "Mechanical properties and microstructure of nano-strengthened recycled aggregate concrete", Nanotechnology Reviews, 11(1), pp. 1499–1510, 2022.
https://doi.org/10.1515/ntrev-2022-0077

[26] Zhang, P., Wei, S., Wu, J., Zhang, Y., Zheng, Y. "Investigation of mechanical properties of PVA fiber-reinforced cementitious composites under the coupling effect of wet-thermal and chloride salt environment", Case Studies in Construction Materials, 17, e01325, 2022.
https://doi.org/10.1016/j.cscm.2022.e01325

[27] Zhang, P., Wang, K., Wang, J., Guo, J., Hu, S., Ling, Y. "Mechanical properties and prediction of fracture parameters of geopolymer/alkali-activated mortar modified with PVA fiber and nano-SiO2", Ceramics International, 46(12), pp. 20027–20037, 2020.
https://doi.org/10.1016/j.ceramint.2020.05.074

[28] Niu, M., Zhang, P., Guo, J., Wang, J. "Effect of Municipal Solid Waste Incineration Fly Ash on the Mechanical Properties and Microstructure of Geopolymer Concrete", Gels, 8(6), 341, 2022.
https://doi.org/10.3390/gels8060341

[29] Li, Y., Zhou, Y., Wang, R., Li, Y., Wu, X., Si, Z. "Experimental investigation on the properties of the interface between RCC layers subjected to early-age frost damage", Cement and Concrete Composites, 134, 104745, 2022.
https://doi.org/10.1016/j.cemconcomp.2022.104745

[30] ASTM "ASTM C469/C469M-22 Standard Test Method for Static Modulus of Elasticity and Poisson's Ratio of Concrete in Compression", ASTM International, West Conshohocken, PA, USA, 2022.
https://doi.org/10.1520/C0469_C0469M-22

[31] Proposed RILEM recommendation "Determination of the fracture energy of mortar and concrete by means of three-point bend tests on notched beams", Materials and Structures, 18(106), pp. 287–290, 1985.
https://doi.org/10.1007/BF02472918

[32] Ojha, P. N., Singh, P., Singh, B., Singh, A., Mittal, P. "Fracture behavior of plain and fiber-reinforced high strength concrete containing high strength steel fiber", Research on Engineering Structures and Materials, 8(3), pp. 583–602, 2022.
https://doi.org/10.17515/resm2022.377ma1228

[33] Das, S., Hoffarth, C., Ren, B., Spencer, B., Sant, G., Rajan, S. D., Neithalath, N. "Simulating the Fracture of Notched Mortar Beams through Extended Finite-Element Method and Peridynamics", Journal of Engineering Mechanics, 145(7), 2019.
https://doi.org/10.1061/(ASCE)EM.1943-7889.0001628

[34] Shah, S. P. "Determination of fracture parameters (KIcs and CTODc) of plain concrete using three-point bend tests", Materials and Structures, 23, pp. 457–460, 1990.
https://doi.org/10.1007/BF02472029

[35] Bažant, Z. P., Pijaudier-Cabot, G. "Measurement of Characteristic Length of Nonlocal Continuum", Journal of Engineering Mechanics, 115(4), 1989.
https://doi.org/10.1061/(asce)0733-9399(1989)115:4(755)

[36] Altheeb, A., Alshaikh, I. M. H., Abadel, A., Nehdi, M., Alghamdi, H. "Effects of Non-Structural Walls on Mitigating the Risk of Progressive Collapse of RC Structures", Latin American Journal of Solids and Structures, 19(3), e440, 2022.
https://doi.org/10.1590/1679-78257023

[37] Ojha, P. N., Singh, B., Singh, A., Patel, V., Arora, V. V. "Experimental study on creep and shrinkage behaviour of high strength concrete", Indian Concrete Journal, 95(2), pp. 30–42, 2021.

[38] Alshaikh, I. M. H., Bakar, B. H. A., Alwesabi, E. A. H., Zeyad, A. M., Magbool, H. M. "Finite element analysis and experimental validation of progressive collapse of reinforced rubberized concrete frame", Structures, 33, pp. 2361-2373, 2021.
https://doi.org/10.1016/j.istruc.2021.06.008

[39] Alwesabi, E. A. H., Bakar, B. H. A., Alshaikh, I. M. H., Zeyad, A. M., Altheeb, A., Alghamdi, H. "Experimental investigation on fracture characteristics of plain and rubberized concrete containing hybrid steel-polypropylene fiber", Structures, 33, pp. 4421–4432, 2021.
https://doi.org/10.1016/j.istruc.2021.07.011

[40] Li, Z. "A Numerical Method for Applying Cohesive Stress on Fracture Process Zone in Concrete Using Nonlinear Spring Element", Materials, 15(3), 1251, 2022.
https://doi.org/10.3390/ma15031251

[41] Arora, V. V., Singh, B., Patel, V., Daniel, Y. N., Mohapatra, B. N. "Stress–Strain Behaviour and Performance Evaluation of High Strength Steel Fibre Reinforced Concrete", Indian Concrete Journal, 93(12), pp. 54–61, 2019.

[42] Arora, V. V., Singh, B. "Durability Studies on Prestressed Concrete made with Portland Pozzolana Cement", Indian Concrete Journal, 90(8), pp. 41–47, 2016.